EUROPEAN SYNCHROTRON RADIATION FACILITY

INSTALLATION EUROPEENNE DE RAYONNEMENT SYNCHROTRON

ESRF

Experiment Report Form

The double page inside this form is to be filled in by all users or groups of users who have had access to beam time for measurements at the ESRF.

Once completed, the report should be submitted electronically to the User Office using the **Electronic Report Submission Application:**

http://193.49.43.2:8080/smis/servlet/UserUtils?start

Reports supporting requests for additional beam time

Reports can now be submitted independently of new proposals – it is necessary simply to indicate the number of the report(s) supporting a new proposal on the proposal form.

The Review Committees reserve the right to reject new proposals from groups who have not reported on the use of beam time allocated previously.

Reports on experiments relating to long term projects

Proposers awarded beam time for a long term project are required to submit an interim report at the end of each year, irrespective of the number of shifts of beam time they have used.

Published papers

All users must give proper credit to ESRF staff members and proper mention to ESRF facilities which were essential for the results described in any ensuing publication. Further, they are obliged to send to the Joint ESRF/ ILL library the complete reference and the abstract of all papers appearing in print, and resulting from the use of the ESRF.

Should you wish to make more general comments on the experiment, please note them on the User Evaluation Form, and send both the Report and the Evaluation Form to the User Office.

Deadlines for submission of Experimental Reports

- 1st March for experiments carried out up until June of the previous year;
- 1st September for experiments carried out up until January of the same year.

Instructions for preparing your Report

- fill in a separate form for each project or series of measurements.
- type your report, in English.
- include the reference number of the proposal to which the report refers.
- make sure that the text, tables and figures fit into the space available.
- if your work is published or is in press, you may prefer to paste in the abstract, and add full reference details. If the abstract is in a language other than English, please include an English translation.

![ESRF logo]	**Experiment title:** *SAXS Imaging of the Bone Nanostructure in Osteoporotic Human Femoral Neck with Micrometer Resolution*	**Experiment number**: SC1200
Beamline: ID13	**Date of experiment**: from: 07.07.2003 to: 11.07.2003	**Date of report**:
Shifts: 9	**Local contact(s)**: Manfred Burghammer	*Received at ESRF:*

Names and affiliations of applicants (* indicates experimentalists):

Himadri Shikhar Gupta*
Wolfgang Wagermaier*
Paul Roschger*
Oskar Paris*
Peter Fratzl

Report:

Bone is a hierarchically structured connective tissue, whose exceptional mechanical properties depend crucially on the structural tissue design at the micron and sub micron level. At these length scales, compact or cortical bone (which is found in the cylindrical shells of most long bones in vertebrates) consists of cylindrically wrapped sheets (lamellae) that wrap around blood vessels and vascular channels (Haversian systems) which provide nutrients and structural components to the growing and differentiating regions in bone. A unit consisting of the cylindrical lamellar shells and the enclosed vascular channel is called an *osteon*, and its mechanical properties are crucial to the structural stability of the entire bone [1].

The lamellae themselves consist of several subunits [2], which contain arrays of mineralized collagen fibrils in the plane of the lamellar sheets. The orientation of the fibrils has been suggested to be longitudinal, transverse as well as at 45° to the osteon long axis [3]. However, very little is known about the actual orientation, shape, and size of the mineral crystallite phase within the lamellae, as well as the spatial variation of the mineral nanostructure between adjacent lamellae and around the osteon[4]. In this experiment we used scanning small-angle X-ray scattering (sSAXS) [5-6]/ scanning wide-angle X-ray diffraction (sWAXD) [7] to characterize the mineral nanostructure with lamellar resolution, using as our test tissue femoral neck sections from healthy human postmenopausal females. The femoral neck is a biomechanically crucial junction in human locomotion, and the site of frequent hip fracture in osteoporosis [8].

Our experiment addressed the following questions :
- Do the mineral particles show uniform or alternating orientations between lamellae, analogous to the alternating lamellae orientation suggested by some authors ?
- What is the spatial variation of the mineral structure (size, shape, thickness and orientation) with increasing radial distance from the center of the osteon ?

- Can SAXS measurements of the same sample at different planar tilt angles to the direct beam enable reconstruction of the full 3D SAXS scattering signal, which is expected to be in the form of ellipsoids of constant intensity in reciprocal space ?

Using specially prepared thin (3 μm) sections of embedded bone from the femoral neck mounted on TEM Cu grids or directly on glass capillaries, a beam diameter of 5 μm, an energy of 13 keV, sample to detector distance 30 mm, and the MAR-CCD detector at ID-13 (with 4×4 binning), we obtained diffraction frames in which both the small angle scatterin signal and the (002) and (310) reflections from the mineral apatite (hexagonal crystal structure) axes were visible (Figure 1). The (310) and (002) axes are orthogonal to each other and their orientation and Debye-Scherrer width gives an estimate of the crystallite size. With a typical measurement time (including detector readout) of 15 seconds, we were able to map regions about 100 μm $\times$ 100 μm around the edge of an osteon within 3 hours.

Figure 2 shows a light microscope image of the osteons and the region scanned (about 1 quadrant of the elliptical osteons). The 2D map of the diffraction frames at each point (5 μm spacing in vertical and horizontal directions) next to the light microscope image shows the SAXS signal at different points. The same region was measured with different tilt angles $\gamma = -55°$, $-35°$, 0, and $+35°$, and scan step size 5 μm $\times$ $\cos(\gamma)$ (to cover the same region).

In Figure 3, the variation of the SAXS signal with γ at the same point is displayed. While the orientation of the ellipse rotates, the ratio of the semi-major to minor axes (eccentricity) does not change significantly. This result indicates qualitatively that the 3D SAXS intensity consists of oblate ellipsoidal (pancake shaped) contours of equal intensity (2 large axes and 1 small axis). The orientation of the long axis of the ellipse, χ_0, may be found from radially integrated intensity plots as a function of azimuthal angle χ (Figure 4).

In order to determine the orientation of the oblate ellipsoidal structure factor in reciprocal space, we define a Cartesian coordinate system (x_1, x_2, x_3), where the beam direction is along x_2 and the detector plane is in the $(x_1 - x_3)$ plane. The normal vector along the thin direction of the oblate ellipsoid was denoted $\mathbf{n} = (\sin(\alpha)\cos(\beta), \sin(\alpha)\sin(\beta), \cos(\alpha))$, where α and β are *a-priori* unknown. Therefore, the orientation of the *long* direction of the ellipsoid with the detector plane is normal to $\mathbf{n}$ and is described by the equation $\tan(\chi_0) = -\tan(\alpha)\cos(\beta+\gamma)$. Since χ_0 is known from Figure 4 and γ is an experimental variable, we can carry out nonlinear fits to obtain α and β. For example, we find that $\beta \approx \pi/2 - 35° = 55°$, since the streak is nearly horizontal ($\chi_0 = 0$) at $\gamma = 35°$. This leads to $\alpha \approx 38°$.

For a full reconstruction of the SAXS ellipsoids, we are currently implementing the following procedure. For a given tilt angle γ, we select an intensity I_0, and characterize the orientation and semi-major and minor axes of the ellipse on which the intensity equals I_0. Repeating the procedure for the different tilt angles and *same* intensity I_0, we obtain a set of points in reciprocal space describing ellipses on the 3D ellipsoid of intensity I_0. Assuming the full ellipsoid is rotated with respect to the laboratory fixed frame by a set of Euler angles (for example the angles α and β used above), we can transform the equation of the ellipsoid from body axes to laboratory axes. The points obtained on the ellipses in the previous step lie on this ellipsoid, and the problem reduces to solving an *overdetermined* set of nonlinear equations, since the number of points we can find on the ellipses is much larger than the 5 unknowns (α and β and the 3 ellipsoid axes) we are solving for. Evaluation of the WAXD data is also in progress, though here the situation is complicated by the curvature of the Ewald sphere, whereby the two peaks of intensity for the (002) reflection (for example) are not equal in height when the *c*-axis is oriented out of the detector plane. Nonetheless, the variation of peak intensities with γ enables reconstruction of the crystallographic orientation of the mineral phase with lamellar resolution.

In summary our results so far are very promising and show that
- Simultaneous SAXS and WAXD combined with scanning microbeam diameters less or equal to than 5 μm, and high flux enables the mineral nanostructure around single osteons to be determined with lamellar resolution.
- Sample tilting around the vertical axis combined with scanning enables reconstruction of the full three-dimensional SAXS scattering intensity and the 3D structure of the WAXD reflections. This

technique thus enables the three-dimensional orientation, shape and size of the mineral particles, and the three-dimensional orientation of the crystallographic axes to be determined with lamellar resolution.

- The initial results suggesting a "pancake" or oblate ellipsoid shaped structure for the SAXS signal oriented at about 40° to the osteons axis suggest that the mineral crystallites have a *fiber texture*, orienting themselves along the collagen fibers (which are also often found oriented along ≈ 45° to the osteons axis), when viewed with lamellar resolution.
- This implies that the mineral crystals spiral around the osteons wall, which may have important biomechanical implications for the natural design of the osteons. We note that similar structures (the cellulose fibrils in wood cell wall) have been found in plants, where the spiral orientation optimizes the extensibility as well as stiffness of the cell wall.

Due to a communication problem between the beamline computers and the MAR-CCD detector belonging to the ID-13 beamline, we were able to start our measurements only at 17:00 on 10.07.2003, thus utilizing only 14 hours of the 72 hours allocated. Nonetheless, we obtained 2 very promising 2D scans around single osteons, and plan to complete the measurements in a second beamtime, applied for the period of Feb – June 2004. In the second beamtime we will include already prepared samples from osteoporotic patients (from the same femoral neck bone type) as well as healthy individuals, in order to obtain better statistics and determine the alterations in bone nanostructure due to diseases and pathological conditions.

[1] J. D. Currey, "*Bones: Structure and Mechanics*", Princeton University Press, Princeton (2002).
[2] S. Weiner and HD Wagner, *Annu Rev Mater Sci* **28**, 271 (1998).
[3] A. Ascenzi, *Bone* **8**, 319–325 (1987).
[4] M. G. Ascenzi et al, *J Struct Biol.* 2003 Jan;**141**(1):22.
[5] P. Fratzl et al., *J. Appl. Cryst.*, **30**, 765 (1997).
[6] I. Zizak et al., *J. Struct. Biol.*, **141**, 208 (2003)
[7] I. Zizak et al., *J. Appl. Cryst.*, **33**, 820 (2000).
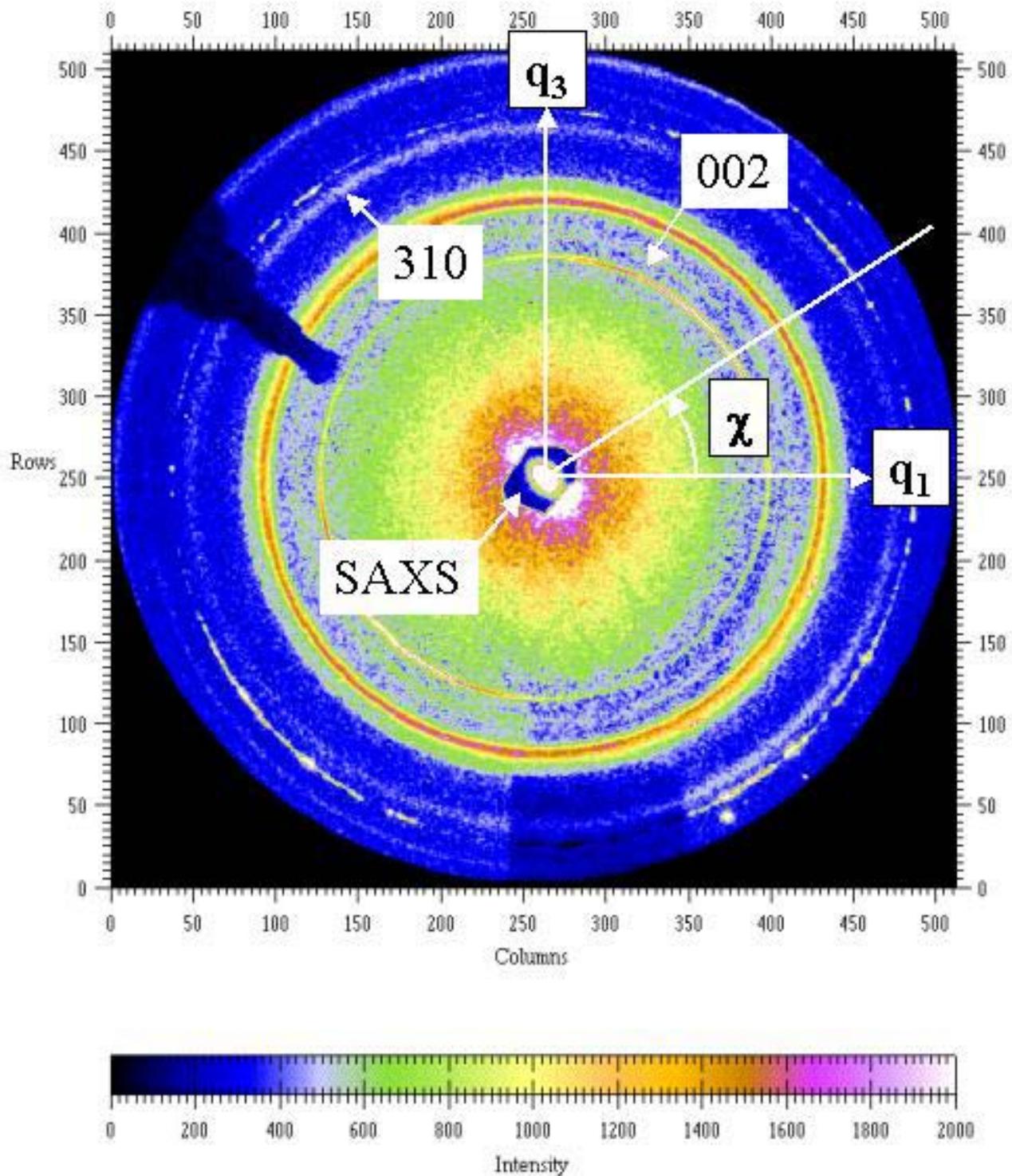[8] K. L. Bell et al., *Bone*, **27**, 297 (2000).

Figure 1: Typical diffraction frame from transverse section of femoral neck bone. The elliptical SAXS signal and the WAXD (002) and (310) reflections are indicated on the figure. Tilt angle $\gamma = -55°$.
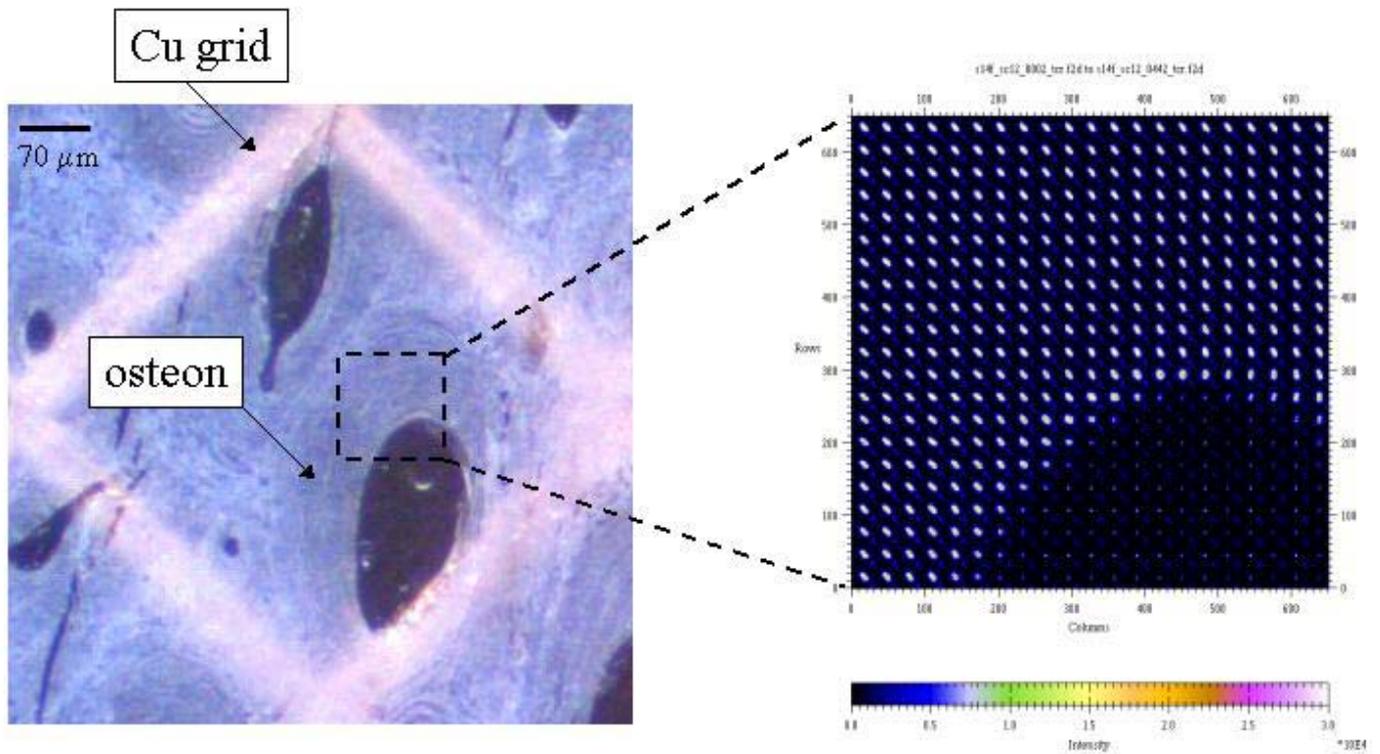
Figure 2: (a) Light microscope image of the transversal bone section used. The osteon is in the center and right of the copper grid unit Region scanned is indicated by a dashed line (b) 2D map of diffraction frames in the region scanned, showing only the SAXS signal in the center of the frame (See Figure 1).
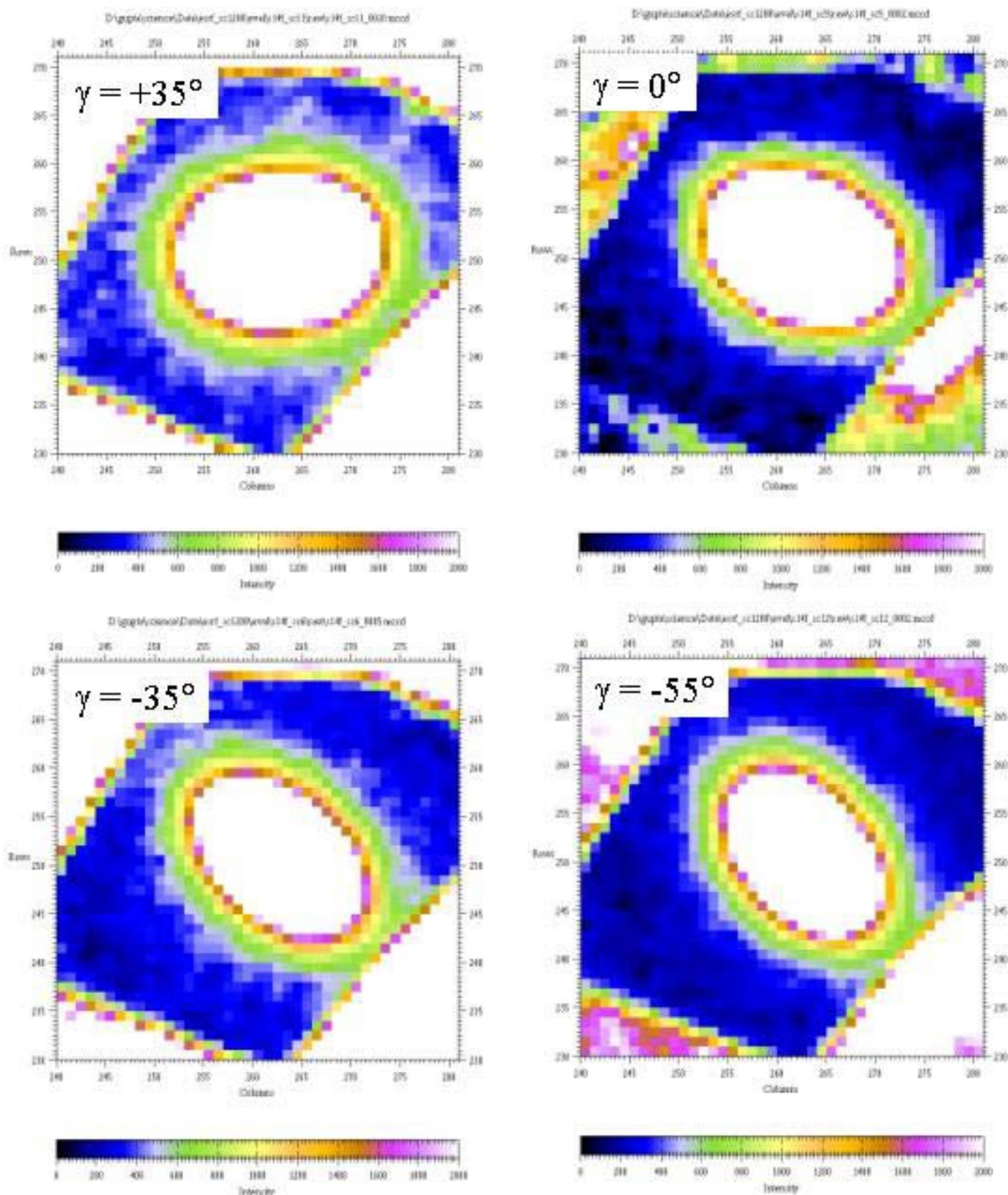
Figure 3: Variation of the SAXS signal for different tilt angles γ. While the principal axes of the ellipse rotate as γ is varied, the eccentricity of the ellipse does not change dramatically.
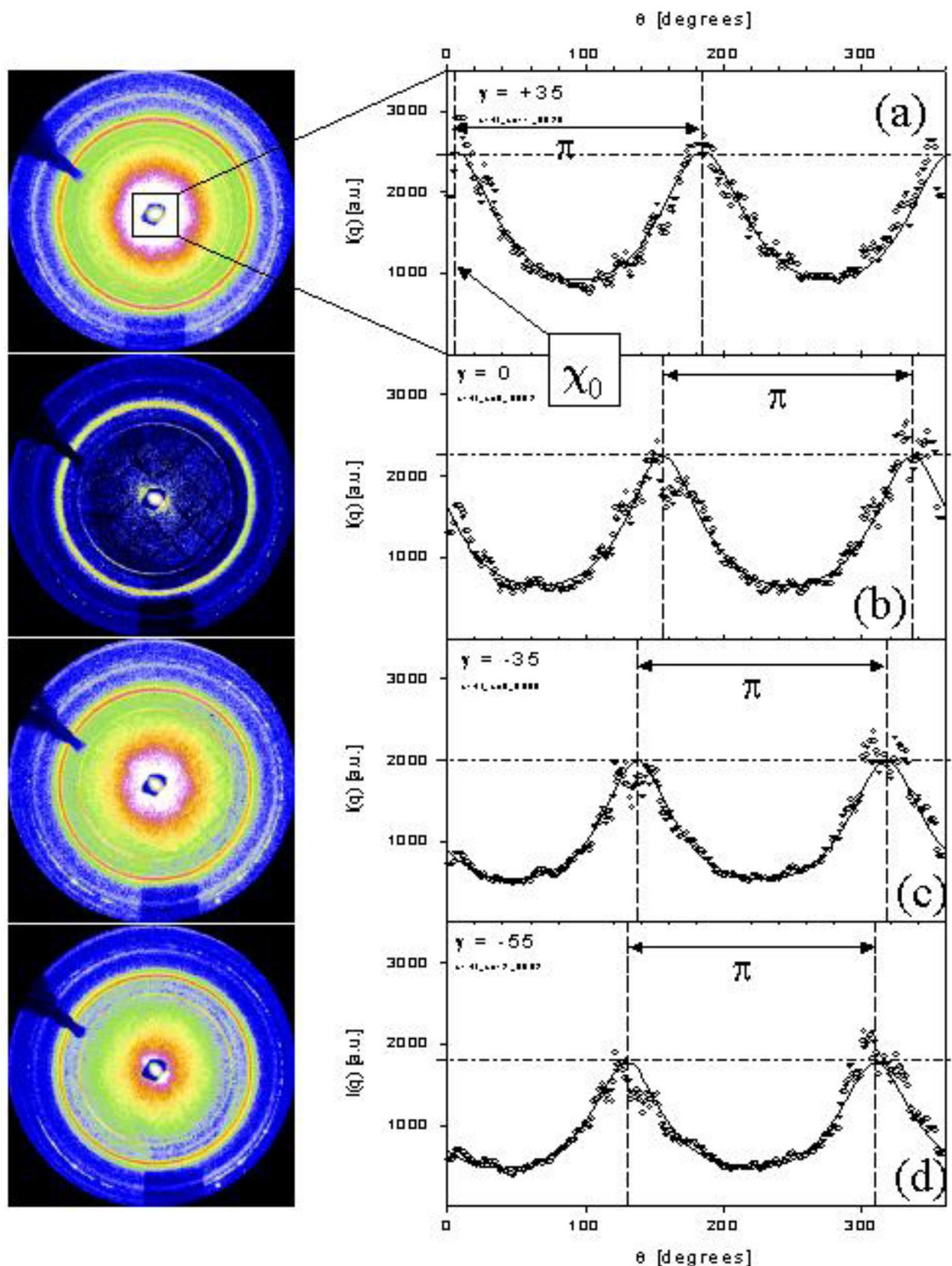
Figure 4: Plots of the azimuthal distribution of the SAXS intensity $I(\chi)$ for different tilt angles γ. As can be seen, the principal axes of the ellipse rotate as γ is varied, resulting in a change of peak position χ_0